JOURNAL OF MATERIALS SCIENCE 25 (1990) 1842–1850

Stable and metastable phase equilibria in the chemical interaction between aluminium and silicon carbide

J. C. VIALA, P. FORTIER, J. BOUIX
Laboratoire de Physico-chimie Minérale 1, U. A. CNRS 116, Université Claude Bernard Lyon 1, 69622 Villeurbanne Cedex, France

An experimental investigation was carried out on the Al–C–Si ternary system under atmospheric pressure and at temperatures up to 1900 K. From the results obtained, a thermodynamic model based on stable and metastable phase equilibria in the Al–C–Si ternary system was set up in order to provide a general description of the chemical interaction between aluminium and SiC. According to this model, aluminium and SiC are in thermodynamic equilibrium at every temperature lower than 923 K. At 923 ± 3 K, i.e. at 10 K below the melting point of pure aluminium, a quasiperitectic invariant transformation occurs in the Al–C–Si system. In this transformation, solid aluminium reacts with SiC to give Al_4C_3 and a ternary (Al–C–Si) liquid phase. The carbon content of this liquid phase is very low; its silicon content is 1.5 ± 0.4 at%. From 923 to about 1620 K, aluminium partially reacts with an excess of SiC, leading to a metastable monovariant equilibrium involving SiC, Al_4C_3 and an aluminium-rich (Al–C–Si) ternary liquid phase, L. The carbon content of this liquid phase, L, remains very low whereas its silicon content increases with temperature from 1.5 ± 0.4 at% at 923 K to 16.5 ± 1 at% at 1620 K. In the temperature range 1670 to 1900 K, two other three-phased monovariant equilibria can be reached by reacting aluminium and SiC. These equilibria involve on the one hand SiC, Al_4SiC_4 and a liquid phase, L′, and on the other hand, Al_4SiC_4, Al_4C_3 and a liquid phase, L″. The former is a stable equilibrium, the latter is a metastable one. At temperatures higher than about 2200 K, the latter metastable equilibrium is replaced by two monovariant stable phase equilibria including the ternary carbide Al_8SiC_7.

1. Introduction

Composite materials consisting either of SiC sintered bodies joined with aluminium or of an aluminium-base matrix reinforced with SiC particles, whiskers or fibres appear as promising candidates for low-weight high-strength applications [1–5]. However, all the technological and theoretical difficulties encountered in the manufacture and use of these materials are not entirely solved. For instance, when these materials are fabricated by liquid-phase infiltration, wettability and chemical interaction are two major problems to be considered [6, 7].

The wettability of SiC by aluminium or aluminium alloys determines the ability for the molten metal to penetrate the pores of SiC fibre tows or preforms: the better the wettability, the lower the infiltration pressure and the higher the interfacial work of adhesion [6]. The chemical interaction at the metal–ceramic interface is responsible for the degradation of the reinforcing whiskers or fibres and for the growth of brittle intermediate phases: it has thereby a determinant influence on the mechanical properties and the corrosion resistance of the resulting composite [7]. A thorough understanding of these interfacial phenomena is then of primary interest for improving the elaboration conditions and the properties of Al–SiC composites. The wettability of SiC by aluminium or aluminium alloys has been the subject of recent investigations [8–10]. The present work is focused upon the chemical interaction problem.

For a long time, it has been commonly accepted that SiC was not attacked by aluminium. In fact, SiC crucibles have been currently used for the melting of aluminium or its alloys. Similarly, a thin SiC coating has been deposited on to boron fibres in order to prevent fibre–matrix interaction in Borsic–aluminium composites [11]. It is now established that SiC can react with molten aluminium, producing Al_4C_3 and silicon, according to the following reaction

$$4Al + 3SiC \rightarrow Al_4C_3 + 3Si \quad (1)$$

Silicon formed in this reaction dissolves in unreacted aluminium, giving rise to an Al–Si liquid alloy [1, 12–17]. In a recent work, we showed that under high pressure (1800 to 2000 MPa), the above reaction could proceed not only from molten aluminium but also from solid aluminium, down to temperatures as low as the eutectic point of the Al–Si binary system [18]. On the other hand, firing Al–SiC mixtures at normal or moderate pressures and at temperatures higher than about 1650 K produces Al_4SiC_4 instead of Al_4C_3

0022–2461/90 $03.00 + .12

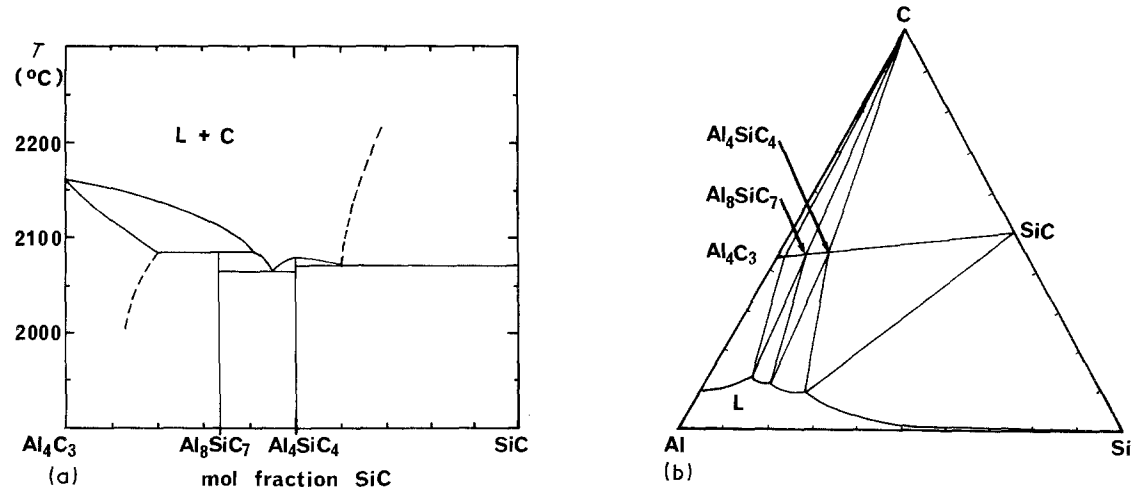

Figure 1 (a) Al_4C_3–SiC isopleth and (b) 2273 K isothermal section of the Al–C–Si phase diagram, according to Oden and McCune [27].

[19–25]. At still higher temperatures, Al_8SiC_7 has also been synthesized [26, 27]. Formation of these ternary compounds at high temperature can be easily understood by considering the Al_4C_3–SiC isopleth and the 2273 K Al–C–Si isothermal section recently reported by Oden and McCune [27] (Figs 1a and b). These high-temperature phase equilibria cannot, however, explain the experimental results obtained when SiC and aluminium react at medium or low temperatures.

Further experiments were then undertaken in the temperature range 300 to 1900 K in order to provide, in terms of stable and metastable phase equilibria, a general description of the thermodynamic aspect of the chemical interaction between aluminium and SiC.

2. Experimental procedure

Mixtures of varying composition were prepared from the following commercial powders (Alfa Ventron): aluminium powder 99%, grain size $< 400\,\mu m$; silicon powder 99.5%, grain size $< 50\,\mu m$; SiC powder 99.8%, grain size $< 50\,\mu m$, α-hexagonal high-temperature variety (mainly 6H and 8H polytypes). In order to reduce the SiO_2 and silicon contamination, the SiC powder was preliminary treated in an aqueous solution containing HF + HNO_3, rinsed and dried.

These mixtures were ball-homogenized for 20 min in a steel mortar and cold pressed at 340 MPa in the form of cylindrical pellets (12 mm diameter, 5 mm high) or of parallelipipedic rods (30 × 5 × 5 mm). Isothermal heat treatments were performed according to three different techniques:

(i) in preliminary experiments, pellets placed on a water-cooled crucible were heated up to 1300 K by electron bombardment under a vacuum of 10^{-3} Pa;

(ii) for quantitative analyses, rods contained in Al_2O_3 crucibles were placed inside quartz tubes sealed under 1 atm purified argon. These rods were then fired up to 1400 K in a conventional vertical tube furnace supplied by a stability controller;

(iii) at higher temperatures ($1400 < T < 1900$ K), rods were introduced into cylindrical Al_2O_3 crucibles, surrounded by a graphite susceptor and r.f.-heated in a vertical quartz tube under a stream of purified argon at a pressure of 1 atm.

When conventional heating was used, temperatures were determined with an accuracy better than ± 5 K. When the mixtures were r.f.-heated, temperatures were read by optical pyrometry and corrected, taking into account the results of a previous calibration carried out with a Pt/90% Pt–10% Rh thermoelectric couple: in that case, the estimated accuracy was about ± 25 K at 1400 K, altering to ± 50 K near 1850 K.

At the end of the heat treatment, the samples were quenched, either by turning off the power supply of the r.f. or electron-beam assembly, or by dropping the sealed quartz tubes into cold water.

Phases produced in the heat-treated samples were characterized by X-ray powder diffraction techniques (two-circle goniometry, Debye–Scherrer and Guinier techniques) using the filtered CuKα radiation (XRD). In order to provide more detailed information about the localization of the reaction products, the extent and morphology of the reaction zones, diamond-polished sections of the samples were examined by optical microscopy (OM) and scanning electron microscopy (SEM). Further characterization was performed by electron microprobe analysis (EMA), using a Cameca Camebax microprobe equipped with a wavelength dispersive spectrometer and an energy dispersive Tracor Northern 2000 analyser. An accelerating voltage of 5 kV, a regulated beam current of about 40 nA and a counting interval of 10 sec were selected as standard operating parameters. In every case, these counting rates were corrected for background.

The silicon content in the aluminium-base matrix of the reacted samples was determined by two different techniques. For samples with a low volume fraction of SiC, large particle-free areas were visible in the polished sections. Therefore, analyses could be performed by EMA, using a broad field scan mode: the counting rates for aluminium and silicon were recorded from 5 to 15 separate areas (0.2 to 1 mm^2), corrected for background, averaged and referred to a calibration curve previously established in the same conditions for Al–Si standard mixtures (Fig. 2). This calibration procedure was preferred to a classical ZAF correction, Al–Si alloys being two-phased mixtures with a non-uniform distribution of the silicon and aluminium grains. The accuracy of the results obtained in this way was observed to be about ± 1 at% for silicon

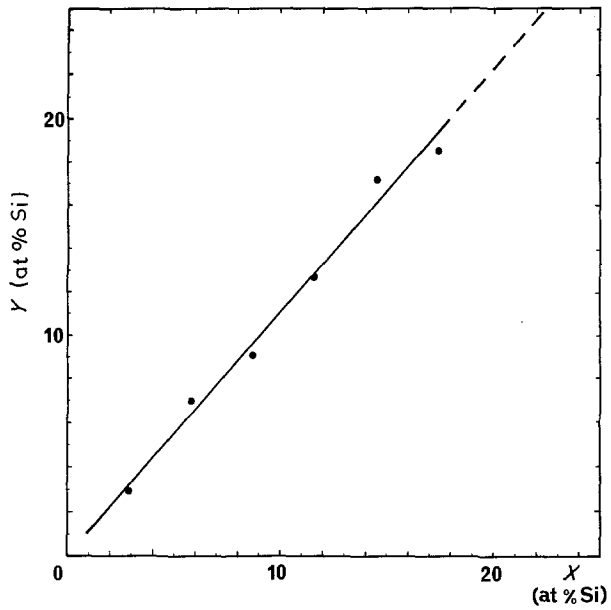

Figure 2 Calibration curve established for the determination of the silicon content in Al–Si alloys by EMA. X, composition of Al–Si standard mixtures; Y, Si/(Si + Al) EMA counting rate ratio.

contents in the range 2 to 15 at % and about ± 2 at % for the highest values (more than 15 at %). Complementary analyses were done by plasma emission spectometry after having dissolved the samples in acidic (HF + HNO_3) or alkaline (NaOH) solutions. As the dissolution was quite hazardous, the accuracy of the results obtained in that way was very difficult to estimate. Then, only the precision of the spectrometric technique could be evaluated: it was of the order of ± 1 at %.

3. Experimental results

3.1. Characterization of the phases produced by reacting aluminium and SiC

In a first series of experiments, cold-pressed mixtures of SiC and aluminium or Al–Si powders containing more than 40 mol % SiC were reacted for varying times at temperatures ranging from 600 to 1900 K. Characterization of the resulting samples led to the following results.

At every temperature lower than 920 K, no reaction could be observed between solid aluminium (m.p. = 933 K) and SiC, even when the heat treatment time was very long. As an example, Fig. 3a shows the XRD spectrum obtained from a sample fired at 840 K for 1200 h: only the two starting phases aluminium and SiC are revealed. A photomicrograph of this sample is shown in Fig. 4. It shows α-SiC particles dispersed in a single-phase aluminium matrix having the typical appearance of a sintered metal powder. The SiC particles exhibit clear-cut outlines and no reaction product can be seen at the Al–SiC interface. Further analysis of this sample by EMA revealed the same silicon content in the bulk of the aluminium matrix as in the starting metal powder (0.1 to 0.3 at %), without any detectable variation in the regions very close to the Al/SiC interface (1 to 3 μm).

In contrast to the foregoing results, reaction products were readily observed by XRD in Al–SiC

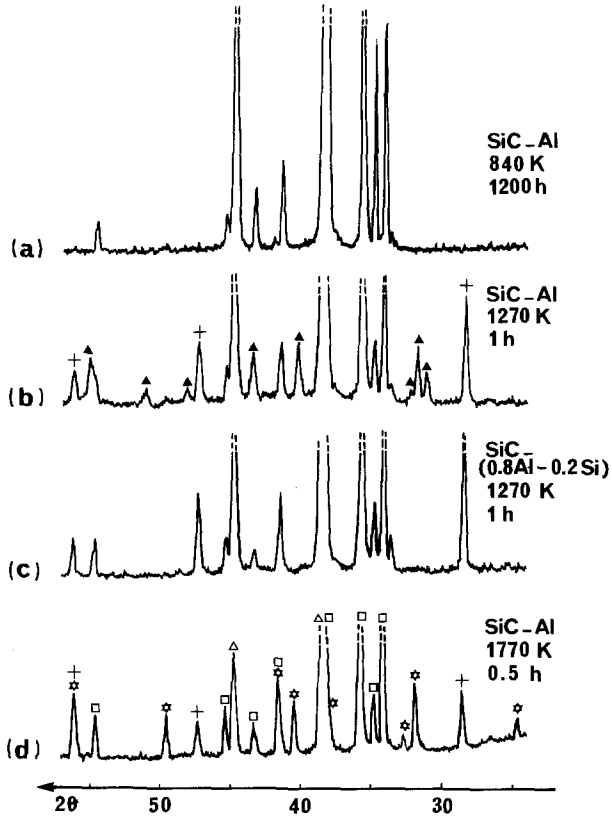

Figure 3 Typical XRD spectra of Al–SiC samples reacted at different temperatures. (△) Al, (□) SiC, (+) Si, ((▲) Al_4C_3, (✪) Al_4SiC_4.

samples heat-treated at temperatures higher than 940 K for only 0.1 to 2 h, as shown by Figs 3b and c.

In the temperature range 940 to 1620 K, Al_4C_3 and silicon were produced (Fig. 3b) according to Reaction 1 (see Section 1). This reaction was observed to proceed quite fast: for example, Al_4C_3 could be easily detected in an Al–SiC specimen heated at 1150 K for only 5 min. An optical photomicrograph of this sample is shown in Fig. 5. Unlike the former case, the SiC particles exhibit jagged outlines. Al_4C_3 forms dark crystallites non-uniformly distributed on the surface of the SiC particles. The metal matrix has the typical appearance of a hypoeutectic Al–Si alloy with large aluminium primary crystals embedded in a fine Al–Si eutectic.

Increasing the temperature or the reaction time

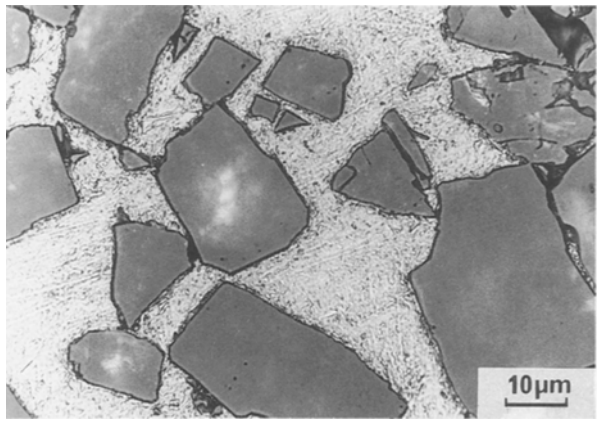

Figure 4 Optical micrograph of an Al–SiC sample heat-treated at 840 K for 1200 h.

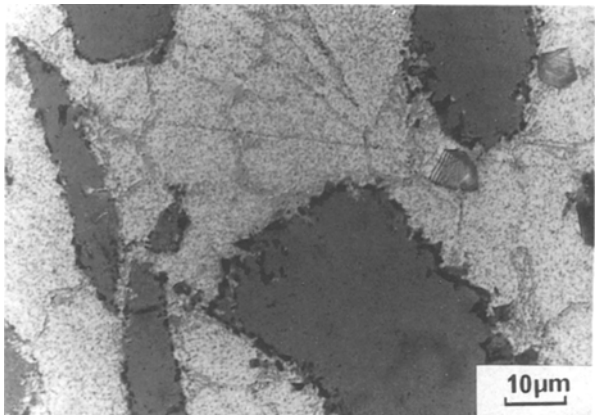

Figure 5 Optical micrograph of an Al–SiC sample heated for 5 min at 1150 K.

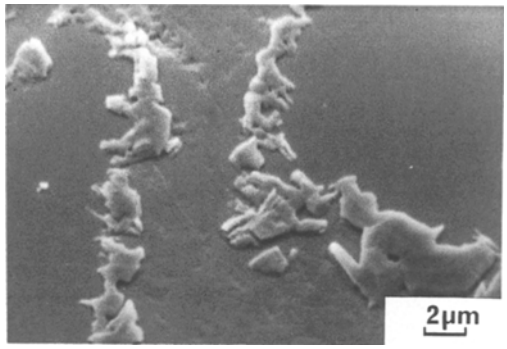

Figure 7 Scanning electron micrograph of the Al/SiC interface in a sample reacted for 1 h at 1270 K.

resulted in the production of greater amounts of Al_4C_3 and silicon. This is illustrated by the photomicrograph presented in Fig. 6, which corresponds to an Al–SiC sample heated at 1270 K for 1 h. In that case, the metal matrix has the typical appearance of a slightly hypereutectic Al–Si alloy. Al_4C_3 crystallites are bigger than previously and tend to join together, forming a reaction zone with an average thickness of about 3 μm on to the surface of the jagged shape SiC particles. Although thicker than previously, this reaction zone still remains discontinuous and small notches in which SiC is in close contact with the Al–Si alloy can be observed. The non-uniformity of the Al_4C_3 layer and the well-facetted character of the constituting crystallites are clearly visible in the scanning electron micrograph shown in Fig. 7.

The particular morphology of the reaction zones revealed by the foregoing micrographs indicates that reaction 1 does not proceed "layer by layer", but via a dissolution–recrystallization process. In this process, the aluminium-base liquid phase is saturated with carbon dissolving from SiC while some Al_4C_3 seeds, formed on the surface of SiC at the beginning of the interaction, grow from the solution. This implies that carbon migrates by liquid-phase diffusion. As far as this process is concerned, Al_4C_3 formed by reaction on the surface of the SiC particles does not efficiently protect these particles from further consumption, as would a good diffusion barrier. Therefore, if thermodynamically possible, Reaction 1 should go to completion. This was actually the case when SiC was heated at 1300 to 1500 K in a large excess of pure aluminium (less than 10 mol % SiC). However, starting from Al–SiC mixtures with an SiC content higher than 40 mol %, unreacted SiC was always found in the reacted samples, whatever the heat-treatment time and whatever the temperature (in the range 940 to 1620 K). Moreover, when a sufficient quantity of silicon was added to aluminium prior to firing, SiC was no longer attacked, as shown by Figs 3c and 8. Finally, heating mixtures of Al_4C_3 and silicon at temperatures higher than 1000 K resulted in the formation of β-SiC and of a liquid phase containing aluminium and silicon. Thus, it must be concluded that interaction between aluminium and an excess of SiC in the temperature range 940 to 1620 K results in a three-phased equilibrium involving unreacted SiC, Al_4C_3 and a carbon-poor (Al–C–Si) liquid phase, L. This equilibrium can be written as follows

$$L \rightleftharpoons Al_4C_3 + SiC \qquad (2)$$

When Al–SiC mixtures were reacted at temperatures higher or equal to 1670 K, the ternary carbide Al_4SiC_4 was observed to be formed instead of Al_4C_3 (Fig. 3d), according to the chemical reaction

$$4Al + 4SiC \rightarrow Al_4SiC_4 + 3Si \qquad (3)$$

As shown by Fig. 9, Al_4SiC_4 mainly appears in the form of large platelets spreading in the liquid phase

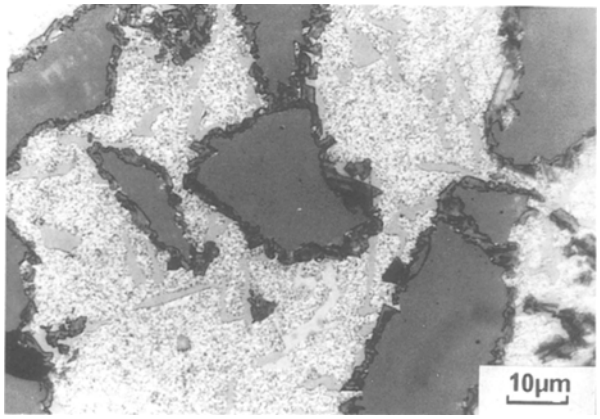

Figure 6 Optical micrograph of an Al–SiC sample after reaction for 1 h at 1270 K.

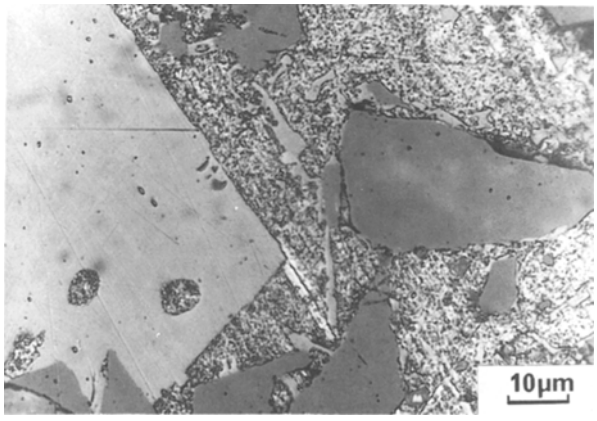

Figure 8 Optical micrograph of SiC particles heated for 1 h at 1270 K in the presence of an Al–Si alloy containing 20 mol % Si. SiC (dark grey) is not attacked under these conditions.

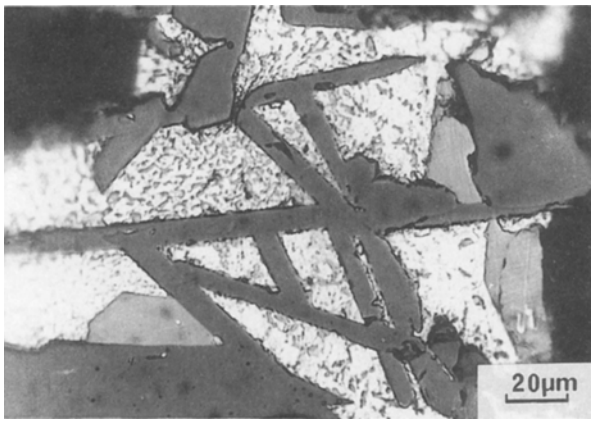

Figure 9 Al_4SiC_4 platelets formed by reacting SiC in excess with aluminium for 30 min at 1770 K.

and leaving the surface of SiC particles directly exposed to this liquid phase. This indicates that, like Al_4C_3 crystals, the Al_4SiC_4 platelets are grown by a dissolution–recrystallization mechanism. However, this mechanism is more complex than the former because Al_4C_3 is transiently formed in an early stage of the reaction. Moreover, the presence of Al_4SiC_4 domains inside some SiC particles suggests that the growth of this ternary carbide may also proceed by solid state diffusion.

Like Reaction 1, Reaction 3 was observed to be incomplete in every case where the initial Al–SiC mixture contained more than 40 mol % SiC. On the other hand, when the initial Al–SiC mixture was SiC-poor (less than 10 mol %), the latter was entirely converted into Al_4SiC_4 and Al_4C_3. Thus, two different three-phase equilibria can be reached in the temperature range 1670 to 1900 K. They can be formulated as follows

$$L' \rightleftharpoons SiC + Al_4SiC_4 \quad (4)$$

$$L'' \rightleftharpoons Al_4SiC_4 + Al_4C_3 \quad (5)$$

Equilibria 3, 4 and 5 involve three condensed phases. Therefore, they are monovariant at a constant pressure, which means that the compositions of the liquid phases L, L′ and L″ only depend on the temperature. These compositions were measured experimentally, after having evaluated the duration to the attainment of equilibrium.

3.2. Equilibrium $L \rightleftharpoons Al_4C_3 + SiC$

Al-SiC mixtures (50 mol % SiC) were reacted for different times at 941 and 987 K. The silicon content, ϱ, in the aluminium matrix was then determined by plasma emission spectrometry after acidic dissolution of the sample. The molar ratio α of SiC converted into Al_4C_3 was deduced from ϱ according to the equation

$$\alpha = 4\varrho/(3 + \varrho) \quad (6)$$

The results plotted in Fig. 10 show that under our experimental conditions, equilibrium is reached after a transient period, the duration of which rapidly decreases when the temperature increases: at 941 K, attainment of the equilibrium takes about 200 h while only 50 h are needed at 987 K.

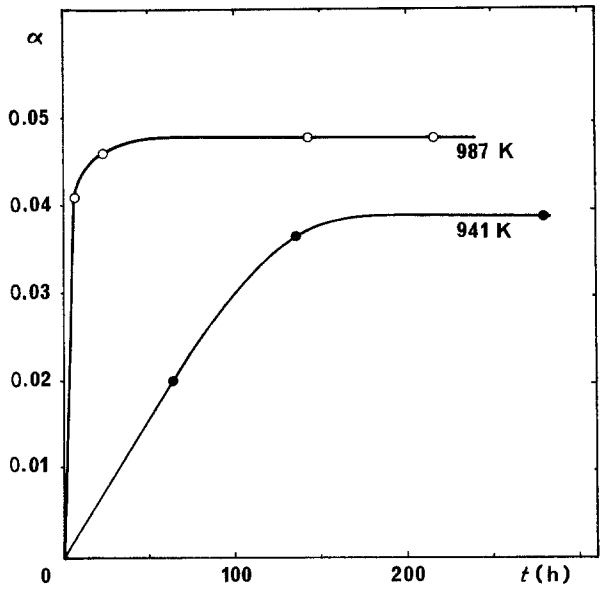

Figure 10 Molar ratio, α, of SiC converted to Al_4C_3 for Al–SiC samples with 50 mol % SiC reacted at 941 and 987 K for different times.

Taking these data into account, Al–SiC samples containing 50 mol % SiC were reacted to equilibrium at temperatures ranging from 923 to 1570 K. After quenching, the resulting samples were analysed by plasma emission spectrometry or EMA in order to determine the silicon content, γ, of the liquid phase, L. Complementary experiments were performed by heating at 1370, 1470 and 1570 K mixtures of SiC particles with Al–Si alloys having a known initial silicon content. The latter specimens were examined by optical metallography in order to evaluate the alloy composition for which Al_4C_3 began to form: this resulted in high and low limits for γ at the three temperatures considered.

The results of these two experimental approaches are summarized in Fig. 11. It can be seen that the silicon content, γ, of the liquid phase, L, in equilibrium with Al_4C_3 and SiC regularly increases with the temperature, from 1.5 ± 0.4 at % at 923 K to 16 ± 0.6 at % at 1570 K. It can be noticed that plasma emission spectrometry leads to highly scattered results, which may be explained by the difficult chemical dissolution of silicon-rich Al–Si alloys. Otherwise, the presence of carbon in the liquid phase, L, could not be evinced by EMA.

3.3. Equilibria $L' \rightleftharpoons SiC + Al_4SiC_4$ and $L'' \rightleftharpoons Al_4SiC_4 + Al_4C_3$

Al–SiC and (Al–Si)–SiC mixtures with appropriate initial compositions were reacted to equilibrium in the temperature range 1670 to 1900 K. Attainment of the equilibria took about 30 min at 1670 K and less than 15 min above 1800 K. After quenching, the resulting samples were analysed by EMA. The silicon content in the liquid phase, L′, in equilibrium with SiC and Al_4SiC_4 was found to be of 17 ± 2 at % at 1740 ± 20 K and of 20 ± 2 at % at 1870 ± 50 K. At the two former temperatures, the silicon content in the liquid phase, L″, in equilibrium with Al_4SiC_4 and Al_4C_3 was of 17.8 ± 2 at % and of 16.3 ± 2 at %, respectively.

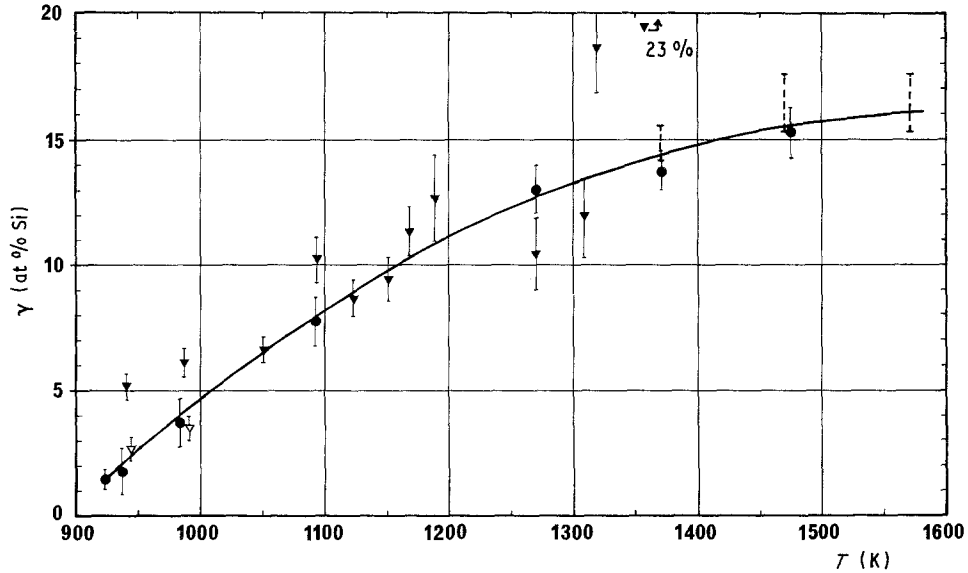

Figure 11 Variation with temperature of the silicon content in the liquid phase, L, in equilibrium with Al_4C_3 and SiC. (●) Analyses performed by EMA; (△, ▲) plasma emission spectrometry after acidic (△) or alkaline dissolution of the metal matrix; dotted vertical segments, metallographic evaluation on (Al–Si)–SiC specimens.

Evidence for the presence of carbon in the liquid phases L′ and L″ were brought by metallographic examination of specimens reacted at high temperature. Indeed, thin Al_4C_3 platelets were observed in the bulk of the metal matrix. From the relative abundance of these platelets, grown on rapid cooling by out-of-equilibrium crystallization from the melt, the carbon content of the liquid phases L′ and L″ was estimated to be in the order of 1 at % near 1800 K.

3.4. Differential thermal analysis

Measurements by differential thermal analysis (DTA) were undertaken on Al–SiC and (Al–Si)–SiC mixtures in the temperature range 300 to 1200 K (Setaram M4 microanalyser). Fig. 12 summarizes the results obtained on heating:

(i) for mixtures containing SiC and pure aluminium, only one symmetrical endothermic peak was observed at 923 ± 3 K;

(ii) for mixtures consisting of SiC and Al–Si alloys (3 to 10 at % of silicon), a symmetrical endothermic peak appeared at 849 ± 1 K. Moreover, two other asymmetrical endothermic peaks were observed below and above 923 K, the difference in temperature between these two peaks increasing with the silicon content of the starting alloy.

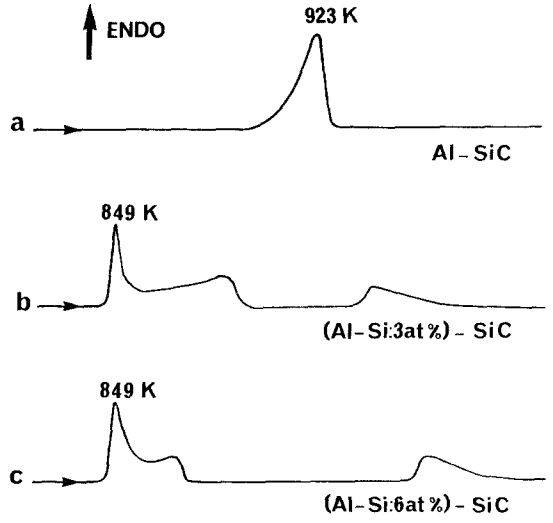

Figure 12 Thermographs recorded for Al–SiC and (Al–Si)–SiC specimens at a heating rate of 4 K sec^{-1}.

From these results, it can be assumed that the symmetrical peaks at 849 K and 923 K correspond to invariant transformations, whereas the asymmetrical peaks may be attributed to monovariant transformations. However, as the thermal effects observed on heating were not fully reversible on cooling, further studies by DTA were not pursued.

4. Discussion

From the foregoing results, it appears that reacting Al–SiC mixtures for a sufficient time at temperatures lower than 1900 K generally leads to two- or three-phased equilibria that obey the rules of thermodynamics and more especially the phase rule. However, these phase equilibria are different from those that should be attained at higher temperatures, according to the Al–C–Si isothermal section established by Oden and McCune [27] and shown in Fig. 1b. This discrepancy, which is due to the fact that the ternary carbides Al_4SiC_4 and Al_8SiC_7 are not formed at low temperature, may be explained either by thermodynamics or by kinetics.

The thermal stability of Al_4SiC_4 and Al_8SiC_7 has been experimentally studied by several authors [20, 22, 26]. In this respect, annealing treatments were carried out on these compounds in the temperature range 1600 to 2200 K. The results were always the same: no evidence of decomposition could be found. Moreover, in a previous work focused on Al_4SiC_4, it was concluded on the basis of experimental evidence and of theoretical considerations that the change in the Gibbs free energy for the formation of this compound from Al_4C_3 and SiC must always be negative below about 2200 K [20]. From these data, the ternary carbides Al_4SiC_4 and Al_8SiC_7 appear as thermodynamically stable phases in the binary subsystem Al_4C_3–SiC,

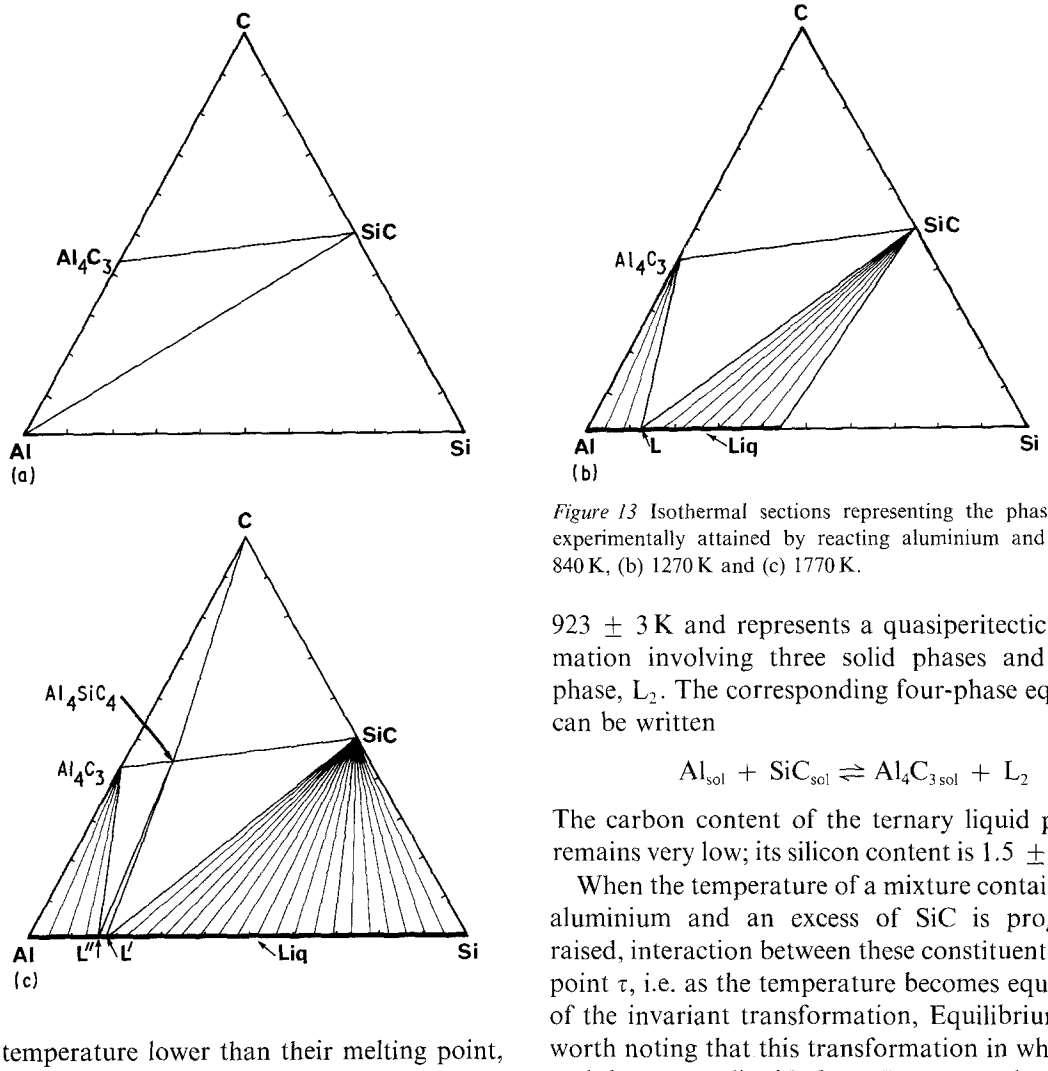

Figure 13 Isothermal sections representing the phase equilibria experimentally attained by reacting aluminium and SiC at (a) 840 K, (b) 1270 K and (c) 1770 K.

at every temperature lower than their melting point, i.e. 2353 and 2358 K, respectively [27].

Consequently, the fact that Al_4SiC_4 and Al_8SiC_7 are not formed when aluminium and SiC react at low temperature does not result from a thermal instability of these compounds but must be attributed to kinetic factors that impede the most stable equilibria to be reached.

Now, as the equilibria actually observed below 1900 K obey the rules of thermodynamics, they can be regarded as metastable equilibria and can thus be represented by metastable phase diagrams.

The more simple of these metastable phase diagrams contains neither Al_4SiC_4 nor Al_8SiC_7. It represents the phase equilibria attained when aluminium and SiC react at temperatures lower than 1620 K. Two typical isothermal sections of this low-temperature phase diagram are reported in Figs 13a and b. Taking into account the DTA results, two invariant transformations must occur in this diagram. These are represented by points E and τ in the polythermal projection of Fig. 14: point E is located at 849 $\pm$ 1 K and corresponds to a eutectic transformation involving three solid phases and a ternary liquid phase L_1. This transformation can be written as follows

$$Al_{sol} + Si_{sol} + SiC_{sol} \rightleftharpoons L_1 \qquad (7)$$

At this point, the silicon content of the liquid phase, L_1, is almost the same as that of the binary Al–Si eutectic, i.e. 12.3 at % [28]; its carbon content is very low (in the p.p.m. range); point τ is located at 923 $\pm$ 3 K and represents a quasiperitectic transformation involving three solid phases and a liquid phase, L_2. The corresponding four-phase equilibrium can be written

$$Al_{sol} + SiC_{sol} \rightleftharpoons Al_4C_{3\,sol} + L_2 \qquad (8)$$

The carbon content of the ternary liquid phase, L_2, remains very low; its silicon content is 1.5 $\pm$ 0.4 at %.

When the temperature of a mixture containing pure aluminium and an excess of SiC is progressively raised, interaction between these constituents starts at point τ, i.e. as the temperature becomes equal to that of the invariant transformation, Equilibrium 8. It is worth noting that this transformation in which Al_4C_3 and the ternary liquid phase, L_2, are produced occurs at about 10 K below the melting point of pure aluminium (m.p. Al = 933 K): then, SiC begins to react with pure aluminium as this metal is still in the solid state. Now, if the Al–SiC mixture is heated for a sufficient time at a temperature higher than 923 K, interaction leads to the three-phased monovariant equilibrium, Equation 2 (see section 3.1). To each temperature between 923 and 1620 K, corresponds a composition for the liquid phase, L, located on the boundary line separating the liquidus surfaces of SiC and Al_4C_3 in the polythermal projection of Fig. 14. The carbon content of this liquid phase, L, increases with the temperature but remains very low. Its silicon content increases regularly with the temperature from 1.5 $\pm$ 0.4 at % at 923 K to 16 $\pm$ 0.6 at % at 1570 K, according to the data reported in Fig. 11.

At temperatures ranging from 1670 to about 1900 K, the ternary carbide Al_4SiC_4 forms by reaction between aluminium and SiC whereas Al_8SiC_7 does not appear. Then, the equilibria experimentally attained in this temperature range can be represented by a "medium temperature" metastable phase diagram including the former compound but excluding the latter. A typical isothermal section constructed at 1770 K in this diagram is reported in Fig. 13c. In the polythermal projection of Fig. 14, this evolution corresponds to the vanishing of the boundary line separating the liquidus surfaces of SiC and Al_4C_3. In its place two new boundary lines appear above

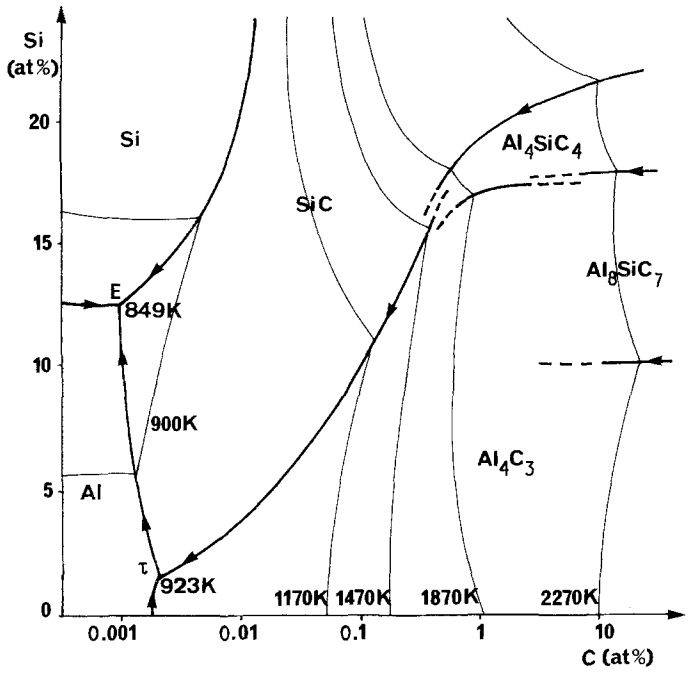

Figure 14 Aluminium-rich part of the liquidus projection of the stable and metastable Al–C–Si phase diagrams.

1670 K: these lines give the composition of the liquid phases L′ and L″ involved in Equilibria 4 and 5 (see section 3.1.).

In the transition range 1620 to 1670 K, out of equilibrium states resulting from the superimposition of the low- and medium-temperature metastable phase diagrams are likely to be observed.

At temperatures higher than 1900 K, a third phase diagram must be used for representing the equilibria attained. Indeed, if the temperature is high enough, Al_8SiC_7 is likely to be found with Al_4SiC_4. This third phase diagram corresponds to that proposed by Oden and McCune [27], an isothermal section of which is presented in Fig. 1b. As the results of these authors were established from experiments performed at very high temperature (more than 2300 K), it can be anticipated that the phase diagram they report represents the stable phase equilibria that can occur in the Al–C–Si ternary system. In the polythermal projection of Fig. 14, the evolution from the medium- to the high-temperature diagram corresponds to the vanishing of the boundary line separating the liquidus surfaces of Al_4SiC_4 and Al_4C_3 and the occurrence of two new boundary lines. As in the former case, out-of-equilibrium states are to be observed between 1900 and about 2200 K. Finally, it can be noticed that the stable high-temperature phase diagram does not include previously reported compounds such as β-Al_4SiC_4 [23] and $Al_4Si_2C_5$ [21], compounds that were not confirmed by further work.

5. Conclusion

The chemical interaction between aluminium and SiC has been experimentally studied under atmospheric pressure over a wide temperature range (300 to 1900 K). As kinetic factors impede the formation of the most stable compounds when the temperature is not high enough, three different Al–C–Si ternary phase diagrams must be considered in order to provide a general description of the thermodynamic aspect of this interaction:

(i) a stable phase diagram representing the equilibria to be really attained at temperatures higher than about 2200 K;

(ii) two metastable phase diagrams describing the equilibria observed at medium temperatures ($1670 < T < 1900$ K) and at low temperatures ($T < 1620$ K).

This thermodynamic model, which is consistent with most of the data previously published on the Al–C–Si system, provides a basis for a better understanding of the interfacial reactions occurring during the manufacture of SiC-reinforced aluminium-base matrix composites.

References

1. T. ISEKI, T. KAMEDA and T. MARUYAMA, *J. Mater. Sci.* **19** (1984) 1692.
2. S. V. NAIR, J. K. TIEN and R. C. BATES, *Int. Met. Rev.* **30** (1985) 275.
3. S. YAJIMA, K. OKAMURA, J. TANAKA and T. HAYASE, *J. Mater. Sci.* **16** (1981) 3033.
4. S. DERMARKAR, *Metals and Materials* **2** (1986) 144.
5. J. C. VIALA and J. BOUIX, *Mater. Chem. Phys.* **11** (1984) 101.
6. F. DELANNAY, L. FROYEN and A. DERUYTTERE, *J. Mater. Sci.* **22** (1987) 1.
7. R. NASLAIN, in "Proceedings of the 1st European Conference on Composite Materials", Bordeaux, France, 24 to 27 September 1985, edited by A. R. Bunsell, P. Lamicq and A. Massiah (European Association for Composite Materials, Bordeaux, 1985) p. 34.
8. T. CHOH and T. OKI, *Mater. Sci. Technol.* **3** (1987) 1.
9. V. LAURENT, D. CHATAIN and N. EUSTATHOPOULOS, *J. Mater. Sci.* **22** (1987) 244.
10. J. P. ROCHER, J. M. QUENISSET and R. NASLAIN, *J. Mater. Sci. Lett.* **4** (1985) 1527.
11. K. PREWO and G. McCARTHY, *J. Mater. Sci.* **7** (1972) 919.
12. J. C. VIALA, P. FORTIER, C. BERNARD and J. BOUIX, *C.R. Acad. Sci. Paris, Ser. 2* **299** (1984) 777.
13. J. C. VIALA, P. FORTIER, C. BERNARD and J. BOUIX, in "Proceedings of the 1st European Conference on Composite Materials", Bordeaux, France, 24 to 27 September 1985, edited by A. R. Bunsell, P. Lamicq and A. Massiah (European Association for Composite Materials, Bordeau, 1985) p. 583.
14. V. M. BERMUDEZ, *Appl. Phys. Lett.* **42** (1983) 70.

15. L. PORTE, *J. Appl. Phys.* **60** (1986) 635.
16. K. KANNIKESWARAN and R. Y. LIN, *J. Met.* **39** (1987) 17.
17. D. J. LLOYD, H. LAGACE, A. McLEOD and P. L. MORRIS, *Mater. Sci. Eng.* **A107** (1989) 73.
18. J. C. VIALA, P. FORTIER, B. BONNETOT and J. BOUIX, *Mater. Res. Bull.* **21** (1986) 387.
19. J. RUSKA, L. J. GAUCKLER and C. PETZOW, *Sci. Ceram.* **9** (1977) 332.
20. J. C. VIALA, P. FORTIER and J. BOUIX, *Ann. Chim. Fr.* **11** (1986) 235.
21. Z. INOUE, Y. INOMATA, H. TANAKA and H. KAWABATA, *J. Mater. Sci.* **15** (1980) 575.
22. P. DORNER, Doctoral Thesis, Stuttgart (RFA), 22 June 1982.
23. V. J. BARCZAC, *J. Amer. Ceram. Soc.* (1961) 299.
24. G. SCHNEIDER, L. J. GAUCKLER, G. PETZOW and A. ZANGVIL, *ibid.* **62** (1979) 574.
25. J. SCHOENNAHL, B. WILLER and M. DAIRE, *J. Solid. State Chem.* **52** (1984) 163.
26. B. L. KIDWELL, L. L. ODEN and R. A. McCUNE, *J. Appl. Crystallogr.* **17** (1984) 481.
27. L. L. ODEN and R. A. McCUNE, *Metal. Trans.* **18A** (1987) 2005.
28. R. P. ELLIOTT, in "Constitution of Binary Alloys", 1st Supplement (McGraw-Hill, New York, 1965) p. 55.

Received 9 December 1988
and accepted 23 August 1989